

Testing the Radiation Hardness of Thick-Film Resistors for a Time-Of-Flight Mass Spectrometer at Jupiter with 18 MeV Protons

D. Lasi, M. Tulej, M. B. Neuland, P. Wurz, T. S. Carzaniga, K. P. Nesteruk, S. Braccini, H. R. Elsener

Abstract—The Neutral and Ion Mass Spectrometer onboard ESA Jupiter mission JUICE employs thick-film resistors (from $\sim 1 \Omega$ to $\sim 1 \text{ M}\Omega$), screen-printed on ceramic elements, to realize high-voltage ion optical elements and decontamination heaters. Despite the relevant space heritage, these materials were never employed before in a radiation environment comparable to Jupiter’s magnetosphere. With this study, we prove the suitability of these materials for the NIM instrument by means of irradiation up to $\sim 16\text{--}85 \text{ Mrad}$ in vacuum with 18 MeV protons. To allow an accurate calculation of the dose, the chemical composition of the samples is determined by Laser Mass Spectrometry. Thanks to a custom-designed irradiation station, the temperature and the electrical parameters of the sample are monitored in real-time during the irradiation, or the sample can be subject to high-voltages representative of the operating conditions in space. All in all, the materials proved to be radiation-hard in the investigated dose range, with few exceptions where permanent damages occur.

Index Terms— Radiation hardening (electronics), Space radiation, Cyclotrons, Thick film circuits, Resistors, Mass spectroscopy, High-voltage techniques, Particle beams.

I. INTRODUCTION

THE JUPITER ICy moons Explorer (JUICE) is a large-class mission of the European Space Agency slated to launch in May 2022 and aimed at studying Jupiter and its three icy moons: Europa, Ganymede, and Callisto. The JUICE spacecraft will spend a significant amount of time inside Jupiter’s intense radiation belts during its three-year long science phase at Jupiter, leading to the accumulation of high-level of Total Ionizing radiation Dose (TID) of $\sim 1.6 \cdot 10^8 \text{ rad Si}$ [1] for basically unshielded elements (0.05 mm Al). Such high doses can be mitigated only partially by reasonable

amounts of shielding; therefore, the radiation hardness of materials employed spacecraft and instruments design must be ensured, either by reference to existing data or by testing.

The Neutral and Ion Mass spectrometer (NIM) [2] is a Time-of-Flight (ToF) mass spectrometer, part of the Nadir Unit (Fig. 1) of Particle Environment Package (PEP) [3], that will investigate the chemical composition of the exosphere of the moons visited by the JUICE spacecraft during multiple flybys and the final orbits around Ganymede. The radiation environment at Jupiter is a design driver both in terms of instantaneous flux and related induced noise at the detector of the instrument [4], [5], [6], and in terms of total dose as far as the electronics of the instrument and, potentially, materials sensitive to radiation are concerned.

The design of NIM employs thick-film resistor technologies that were successfully deployed in previous space instruments designed and manufactured in collaboration between the University of Bern and Empa (Dübendorf), such as RTOF [7] for the Rosetta mission of ESA and NGMS [8] for the Luna-Resurs mission of Roscosmos. Specifically, NIM employs two types of thick-film printed resistors, DuPont Series 2000 ($\sim \text{k}\Omega/\text{sq}$) and 7400 ($\sim \text{m}\Omega/\text{sq}$) [7], for the realization of the high-voltage ion-optical elements of the Ion mirror (IR) [10] and of a decontamination heater hosted inside the Ion Source (IS). The location of these material in the instrument is shown in Fig. 1. The combination of these materials with ceramic substrates is a key technological element for the realization of a lightweight instrument that is compliant to both the performance and the instrument qualification requirements.

Despite the relevant space heritage, these materials were never employed before in space in a radiation environment comparable to Jupiter’s, nor are there data available from previous radiation tests on these resistors for other applications on Earth. Moreover, their detailed chemical

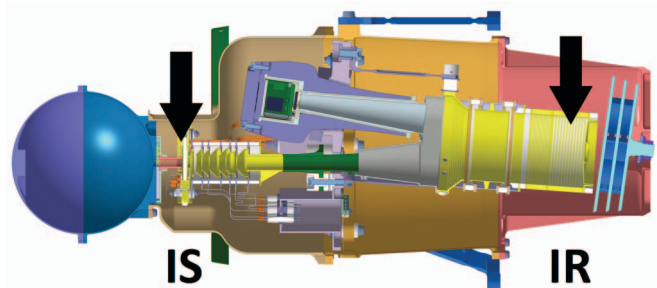


Fig. 1: The sensor of NIM instrument, showing the location of the Ion Source (IS) heater and of the Ion mirror (IR) resistors.

Manuscript received July 11, 2017.

This work was supported by the ESA PRODEX programme.

Davide Lasi, Marek Tulej, Maïke Brigitte Neuland, and Peter Wurz are with Space Research and Planetary Science, Physics Institute, University of Bern, Sidlerstrasse 5, CH 3012 Bern, Switzerland (e-mail: peter.wurz@space.unibe.ch).

Tommaso Stefano Carzaniga, Konrad Pawel Nesteruk, and Saverio Braccini are with Albert Einstein Center for Fundamental Physics, Laboratory for High Energy Physics, Sidlerstrasse 5, CH 3012 Bern, Switzerland (e-mail: saverio.braccini@lhep.unibe.ch).

Hans Rudolf Elsener is with Empa, Swiss Federal Laboratories for Materials Science and Technology, Laboratory for Joining Technologies and Corrosion, CH-8600 Dübendorf, Switzerland (e-mail: HansRudolf.Elsener@empa.ch).

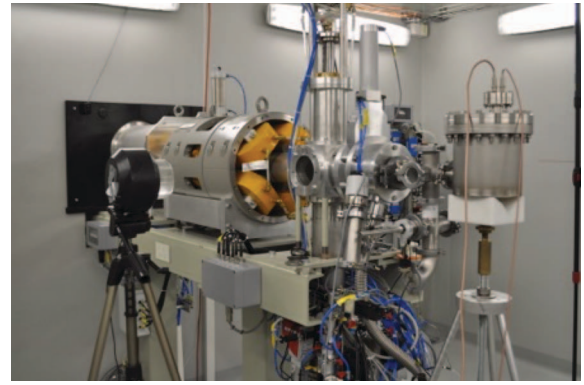


Fig. 2: The medical proton cyclotron with its beam transfer line (BTL) for multi-disciplinary research (left). The experimental area with independent access for radiation hardness studies (right).

composition is not known, so their possible inherent radiation hardness cannot be assessed *a priori*.

To confirm the suitability of the material for the JUICE mission, and more in general for any application where these materials are exposed to very-high radiation doses, we performed an experimental investigation with 18 MeV protons (p^+) at the cyclotron facility [12] of the University of Bern (Inselspital, Fig. 2) over four test sessions. This facility is conceived for radioisotope production for medical imaging and for multidisciplinary research by means of a dedicated beam transport line (BTL), which can deliver currents from ~ 1 pA to ~ 150 μ A for a range of applications [13]. In addition, for the accurate determination of the deposited dose in the samples by means of Monte-Carlo simulations, we have performed semi-quantitative analyses of the samples composition by Laser Mass Spectrometry (LMS) [15]. This study is of utmost importance to confirm that the assumed technological baseline of NIM is compatible with Jupiter environment. Besides, it provides the grounds for envisaging the implementation of lightweight high-voltage ion-optical elements on instruments for high-radiation environments.

II. MATERIALS

DuPont Series 2000 resistors (\sim k Ω / sq) are used for the electrodes of the NIM Ion mirror (IR), and have been previously implemented in the NGMS instrument [8]. They are screen-printed by a dispenser inside a 5 cm-wide ceramic cylindrical structure (the ion mirror), for a resulting resistance in the order of several hundred M Ω , and supplied with up to 5kV to create the desired electrostatic field that repels the ions toward the detector [10]. This design solution allows to fabricate a very lightweight ion optical system, which is necessary to meet the tight mass budget of <1 kg (excluding detector radiation shielding [6]) available for the NIM instrument. Even a moderate variation ($<20\%$) of the sheet-resistivity of the resistor paste may lead to a disruption of the ion-optics of the sensor that cannot be compensated by operating the electrodes at a different voltage. Should these resistors show excessive degradation of their properties at the JUICE mission End of Life (EOL), the design of the NIM instrument would have to be reworked to use discrete metal electrodes, or significant amount of shielding would be necessary around the sensitive ion-optical elements. In either

case, the fixing the problem would come with a significant mass penalty, likely outside the possibilities of the JUICE spacecraft.

DuPont Series 7400 resistors (\sim m Ω / sq) are used for a decontamination heater inside the NIM Ion Source (IS), and have been previously implemented in the NGMS instrument [8]. They are screen-printed onto a small (1.5 x 1.5 cm) ceramic plate that is thermally coupled to the IS structure. The 7499 paste has been already implemented in a similar configuration on a space instrument for the Bepi-Colombo mission to Mercury [11]. By the application of a low-voltage, depending on the actual resistance and target power dissipation, the resistor acts as a heater, raising the IS temperature up to 300 $^{\circ}$ C for removing contaminants accumulated on the ion source that may provide undesirable signals in the mass spectrum. A moderate variation of the heater's resistance due to radiation effects could be compensated by achieving the same power dissipation by applying a higher or lower supply voltage; however, excessive ($>20\%$) variation of the resistance may not be compensated, or lead to a short or an open circuit that makes the heater unusable.

III. END-OF-LIFE TOTAL DOSE

The NIM instrument is mounted on the exterior of the spacecraft and it is fully exposed to the radiation environment. Only the particle detector is shielded against instantaneous fluxes of radiation at Jupiter [6]. Both types of printed resistors are placed in locations of the NIM instrument that are not specifically shielded against radiation, so they happen to be protected only by a moderate line-of-sight thickness of materials that to surround them for structural reasons (Fig. 1).

The equivalent Al-equivalent thickness around DuPont series 2000 is estimated to be ~ 2 mm, mainly provided by the IR walls and the rest of the sensor structure. The equivalent Al-equivalent thickness around DuPont series 7400 is estimated to be ~ 4 mm, provided by the IS elements.

Based on the JUICE mission environmental specifications [1], we derived from the Al-equivalent thickness an EOL TID of 3.8 Mrad Si for DuPont Series 2000 and 1.9 Mrad Si for the DuPont Series 4000. To account for the all the uncertainties of our test method (e.g., testing with protons only and assuming that the results will be valid for the electrons-dominated

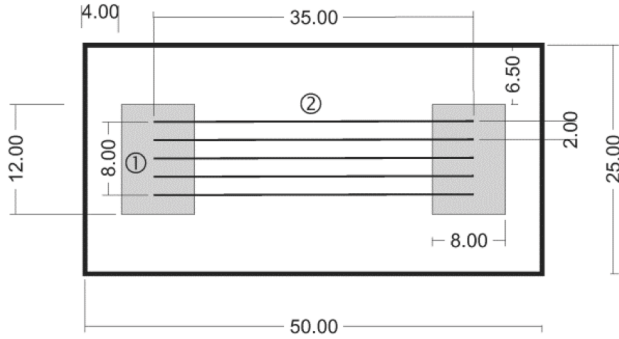


Fig. 3: Geometry of the samples with narrow traces. The bold trace samples have a single ~ 4 mm-wide trace instead of 5 narrow traces.

environment at Jupiter, approximations in the calculation of the dose deposited in the samples) we multiply these doses by a factor of 4 to derive the minimum target dose. It has to be noted that protons deposit also Total Non-Ionizing Dose (TNID), also known as Displacement Damage (DD) dose, and the ratio between TID and TNID is such that, considering the characteristics of the environmental spectrum of energetic particles at Jupiter targeting a TID value result in a large over-testing of TNID. Therefore, this study allows verifying the materials' resistance not only to ionizing, but also to non-ionizing dose effects.

IV. SAMPLES

Several combinations of resistor pastes, substrates, and protection layers are investigated in the present study (Table I). For ease of reference, ion mirror samples are indicated with #R, whereas low-resistivity and high-resistivity heater samples are indicated with #HL and #HH, respectively.

- #R: DuPont 2051 (100 k Ω /sq), lot WHP295 (2012).
- #HL: DuPont 7410 (90–110 m Ω /sq), lot WJE018 (2012).
- #HH: DuPont 7499 (800–1200 m Ω /sq), lot SDE083 (2008).

The paste has been fired in air at 900 $^{\circ}$ C for #R samples and at 850 $^{\circ}$ C for #HL and #HH samples. In all cases, the protection layer has been fired at 950 $^{\circ}$ C.

Two types of samples are investigated: with 5 narrow traces (Fig. 3) and with a single wide trace. The latter are identified with the letter “B” in the samples' ID.

The size of the ceramic substrate is $25 \times 50 \times 0.635$ mm³. The thickness of the paste is between 30 and 45 μ m, which means that the samples are fully traversed by 18 MeV protons.

V. IRRADIATION FACILITY

Radiation hardness tests on the samples are performed using 18 MeV proton beam provided by the medical cyclotron at the University of Bern hospital [12]. This facility is conceived for radioisotope production for medical imaging and for multidisciplinary research by means of a dedicated beam transport line (BTL). Average current densities at the target between ~ 0.5 and ~ 10 nA cm⁻² are delivered for this experiment. Before each irradiation, the beam parameters are optimized aiming at a flat proton distribution at the sample.

TABLE I
SAMPLES (ALL DATA BEFORE IRRADIATION)

Sample ID	DuPont	Substrate	Metallization	Resistance ²
#R-1	2051	Al ₂ O ₃ 96%	CuSnTiZr	10.29 M Ω
#R-2	2051	Al ₂ O ₃ 96%	CuSnTiZr	10.36 M Ω
#R-3	2051	Al ₂ O ₃ 96%	CuSnTiZr	12.43 M Ω
#R-5	2051	Al ₂ O ₃ 96%	CuSnTiZr	16.18 M Ω
#R-B1	2051	Al ₂ O ₃ 96%	CuSnTiZr	920 k Ω
#R-B4 ¹	2051	Al ₂ O ₃ 96%	CuSnTiZr	758 k Ω
#HL-1	7410	Al ₂ O ₃ 99.6%	CuSnTiZr	27 Ω
#HL-B1	7410	Al ₂ O ₃ 99.6%	CuSnTiZr	1.7 Ω
#HL-B4 ¹	7410	Al ₂ O ₃ 99.6%	CuSnTiZr	1.8 Ω
#HH-B2	7499	Al ₂ O ₃ 96%	CuSnTiZr	78.4 Ω
#HH-B3	7499	Al ₂ O ₃ 96%	Incusil-ABA	61.3 Ω
#HH-B4 ¹	7499	Al ₂ O ₃ 96%	Incusil-ABA	55.6 Ω

¹ = sample not irradiated but used for compositional analysis by LMS.

² = as measured by the manufacturer of the printed resistors (EMPA), at 500V.

The profile is measured on-line and non-destructively using a beam scanner – named UniBEAM [14] – in both X- and Y-direction. The beam current was monitored in real-time thanks to a Faraday cup built-in the custom made vacuum enclosure of the samples (Fig. 4).

VI. EXPERIMENTAL METHOD

The electrical properties of the samples are measured before irradiation at contact with the samples using a Megger MIT430 Insulation Tester (high-ohmic samples) or a GWInstek GOM-802 Milli-Ohm Meter (low-ohmic samples). The same measurement is repeated after irradiation.

The samples are placed in a custom-made vacuum irradiation station (Fig. 4), which is attached at the end of the cyclotron beam line. The samples are aligned vertically, because the beam profile in Y is typically flatter than in X (Fig. 6). The chamber is equipped with a sample holder, a 6 mm-thick aluminum block placed behind the samples, an aluminum frame placed before the sample, and four vacuum feedthroughs. The block (area exposed to beam: 900 mm²) act as beam dump and is used to monitor the beam current during irradiation by connecting it to an electrometer (Keysight B2985A). The frame is placed at a bias voltage of about -55 V for secondary electrons suppression.

Two additional vacuum feedthrough are available to monitor the sample temperature with a Pt-1000/100 sensor, to

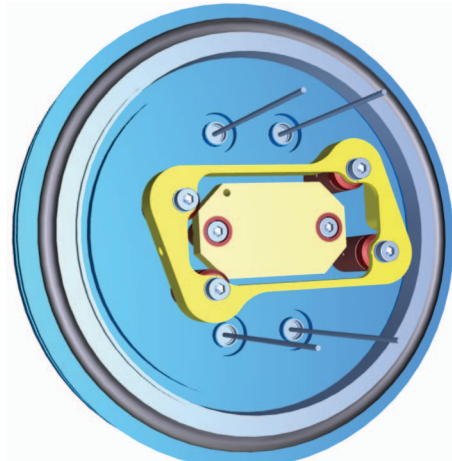


Fig. 4: CAD model of the sample irradiation station, showing both the block placed behind the sample (beam dump) and the frame at bias voltage.

TABLE II
SUMMARY OF SAMPLES IRRADIATION CONDITIONS AND RESULTS

Test Session	Sample ID	Resistance before irradiation [voltage] ³	Average 18 MeV p ⁺ current density (nA cm ⁻²) × time	Actual 18 MeV p ⁺ fluence (# cm ⁻²)	Actual Dose ¹ (Mrad)	Temperature Initial / Final (°C)	Resistance after irradiation [voltage] ³
I	#R-1	10.3-10.4 MΩ [50 V]	3.0 × 30 min	3.4 × 10 ¹³	11.6±1.1	23/42	10.3-10.4 MΩ [57.6 V] 10.3 MΩ [551 V]
II	#R-2	10.4 MΩ [57.9 V] 10.4 MΩ [551 V]	3.8 × 30 min	4.4 × 10 ¹³	15.0±1.5	-	10.4 MΩ [58.0 V] 10.4 MΩ [551 V]
III	#R-3	12.43 MΩ [500 V]	2.8 × 5.5 min + 5.6 × 5 min + 11.0 × 11.5 min + 17.7 × 9.75 min	1.3 × 10 ¹⁴	44.3±4.3	23/120	a) 16.1 MΩ [58.0 V] b) 13.2 MΩ [551 V] c) 13.7 MΩ [57.9 V]
IV	#R-5	16.2 MΩ [58.0 V] 16.2 MΩ [551 V]	11* × 60 min	2.5 × 10 ¹⁴	85±16	-	16.2 MΩ [57.9 V] 16.2 MΩ [551 V]
I	#R-B1	1.04 MΩ [50 V]	3.0 × 30 min	3.4 × 10 ¹³	11.6±1.1	23/42	1.02-1.04 MΩ [57.6 V] 1.00 MΩ [547 V]
II	#HL-1	32.115 Ω	0.4 × 10 min + 1.0 × 10 min + 2.1 × 11 min + 4.3 × 10 min + 11.1 × 4 min	4.7 × 10 ¹³	14.4±1.8	-	31.989 Ω
IV	#HL-B1	1.614 Ω	3.1 × 46 min	5.4 × 10 ¹³	16.6±2.0	-	1.619 Ω
II	#HH-B2	78.83 Ω	0.5 × 10 min + 1.1 × 10 min + 2.2 × 10 min + 4.4 × 10 min + 11.1 × 5 min	5.1 × 10 ¹³	16.3±2.1	-	79.99 Ω
IV	#HH-B3	61.03 Ω	3.1 × 45.5 min	5.2 × 10 ¹³	16.7±2.1	-	65.56 Ω

N/A means "Not Available". ¹ = From SRIM calculation. The standard deviation is based on the uncertainty of the density, which is the largest source of error. ³ = measured at contact. * = initial current value, measured before electrometer was damaged.

apply a high-voltage to the sample (Fug HCN 14-3 500 HV Power Supply; from 0 to +3.5kV), or to read the sample resistance. These readings are performed in real-time during irradiation by means of long cables (~17 m) routed outside the bunker of the BTL. The resistance of the samples in this measurement configuration is different from the value measured at contact because of the effect of the cables.

VII. DOSE TARGET AND ACTUAL DOSE

The p⁺ fluence needed to deposit a dose representative of the JUICE mission's EOL is calculated. Doses up to several Mrad can be delivered in by varying the beam intensity, the fluence and the irradiation time. A typical irradiation of 30 minutes at 10 nA delivers ~100 Mrad on a surface of 1 cm² in aluminum.

Because the samples' chemical composition was unknown before starting the measurements, approximate hand calculation of p⁺ fluxes to deposit the target doses have been performed. As the composition information became available after measurements with Laser Mass Spectrometry [15], the SRIM Monte Carlo code [17] was used to assess the ionization loss inside the irradiated materials.

The samples are irradiated until the desired total accumulated p⁺ fluence is achieved. In some cases, depending on the available beam time and on the sample behavior, a higher fluence is achieved to verify if the material would survive yet higher doses than the one foreseen for this specific application.

VIII. RESULTS

A. Compositional Measurements and Dose Calculation

The result of the analysis performed with LMS are reported in Fig. 5. In the latter, the hypothesized origin or function of each element is indicated.

Based on the output of the composition measurement, three targets are defined in SRIM using the ≥ 1.0 g/100g element from Table II. The density and thickness after firing of the resistor paste is derived from measurements and calculations as follow:

- #R: 3.1±0.3 g/cm³; 12 μm
- #HL: 5.7±0.7 g/cm³; 12 μm
- #HH: 4.7±0.6 g/cm³; 10 μm

The resulting energy deposited by 18 MeV protons in the thin layer of resistor paste printed onto the samples is:

- #R: 0.066 ± 0.007 MeV/p⁺
- #HL: 0.13 ± 0.02 MeV/p⁺
- #HH: 0.094 ± 0.01 MeV/p⁺

The indicated uncertainty of the dose measurement is derived from the uncertainty of the density determination, which is much larger than the sensitivity of the proton energy loss into the material due to the uncertainty of the semi-quantitative mass spectrometric measurement.

The beam profiles for all test sessions are given in Fig. 6. The beam profiles are not calibrated and beam profiling occurred at the beginning of each measurement sessions, sometimes weeks after the previous session; therefore, the absolute scale on the vertical axis is not indicative of the beam intensity.

The beam profile has been optimized to be as flat as possible along the y-axis, that is along the orientation of the tracks of the sample. A good flatness could not be achieved for session III and for the highest current settings of session IV. However, in those sessions we irradiated only samples (#R-3 and #R-5) over-tested far beyond the nominal dose target (Table II). Therefore, for all samples irradiated at the nominal fluence the sample illumination can be considered uniform, without the need of considering the non-uniform density of the protons for interpreting the results (e.g., the

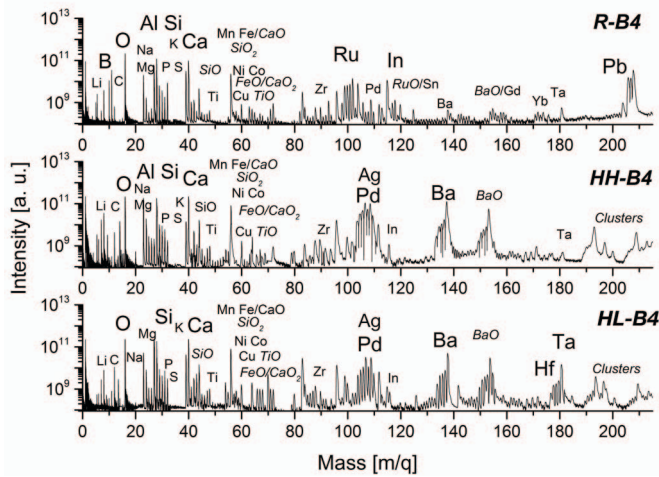


Fig. 5: Mass spectra of the three different resistor pastes #R, #HH, and #HL. sheet resistance degradation, if any, can be considered at sample average level).

B. Ion Mirror (#R, DuPont 2051) Samples Irradiation

The irradiation of #R-1 and #R-B1 samples is performed with constant beam current of $\sim 3 \text{ nA cm}^{-2}$ for 30 min and real-time temperature measurement. The temperature profile (Fig. 9) shows that the samples temperature increases by $\sim 20^\circ \text{C}$, which does not pose any concern since all pastes are fired at very high temperature ($>850^\circ \text{C}$). The temperature profile is substantially equivalent for both the narrow- and the bold-traces samples, thus showing that the trace type does not affect the thermal behavior. Since all samples are printed on almost identical ceramic substrates, we consider this measurement to be indicative of the temperature behavior of all samples irradiated under similar conditions. The resistance of both #R-1 and #R-B1 is unchanged after irradiation (Table II), thus showing no sample degradation up to $\sim 12 \text{ Mrad}$.

#R-2 is irradiated for the same time of #R-1 and with a slightly higher current density of $\sim 4 \text{ nA cm}^{-2}$ for 30 min, with the application of +3.5 kV across the sample. The current of the high-voltage supply, monitored during irradiation, remained constant at 0.34 mA for the first 15 min, and

TABLE II

SAMPLES COMPOSITION MEASUREMENTS (% IN MASS)

Element	#R	#HH	#HL	Hypothesized origin or function
O	65.0*	24.8*	21.4*	Matrix + Metal Oxides
Ca	6.3*	25.9*	8.5*	Matrix
Mg	Traces	0.6	0.1	Matrix
Al	1.9*	Traces	Traces	Matrix
Na	3.0*	0.6	0.7	Matrix
K	1.9*	Traces	1.2*	Matrix
Si	3.8*	7.5*	8.5*	Matrix
Fe	2.4*	9.2*	3.1*	Related to conductivity
Ru	8.7*	Traces	Traces	Related to conductivity
Pb	15.4*	Absent	Absent	Related to conductivity
Ba	0.1	6.6*	10.8*	Related to conductivity
Pd	0.1	11.5*	11.7*	Related to conductivity
Ag	0.1	12.4*	19.2*	Related to conductivity
Hf	Absent	Absent	0.6*	Related to conductivity
Ta	0.2	Absent	2.3*	Related to conductivity
In	4.3*	Traces	0.1	Related to conductivity
Ti, Cu, Sn	Traces	Traces	Traces	Residues of metallization
Zr	0.7	0.1	0.1	Residues of metallization
P	0.5	0.3	0.1	Unknown
S	0.3	0.1	0.1	Unknown

Values are % in mass (g/100g). "Traces" indicates $<0.1\%$ elements. Error on data is $\pm 20\%$. (*) = used to define the target in SRIM.

changed to 0.35 mA for the last 15 min. This sample too does not show any variation in the measured resistance before and after irradiation (Table II), thus demonstrating radiation hardness until $\sim 15 \text{ Mrad}$.

Because the first three samples did not show appreciable variation of their properties by irradiation to 12–15 Mrad, two additional samples are irradiated at much higher doses and currents, one with temperature measurement and one with an applied high-voltage, to see if radiation damages could be observed at extreme dose levels.

#R-3 is irradiated with different steps of increasing beam current (Fig. 10) from ~ 3 to $\sim 18 \text{ nA cm}^{-2}$, for a total dose of $\sim 44 \text{ Mrad}$. The current density steps can be appreciated as a variation in the slope of the cumulative fluence curve and in the transition to a different thermal profile in Fig. 10. As the sample temperature is increasing to 100°C and beyond, so the risk of outgassing increases, the beamline pressure is monitored. The sample starts to outgas during the last beam current ramp at $\sim 18 \text{ nA cm}^{-2}$, where both a dent in the temperature profile and an increase in the beamline pressure is

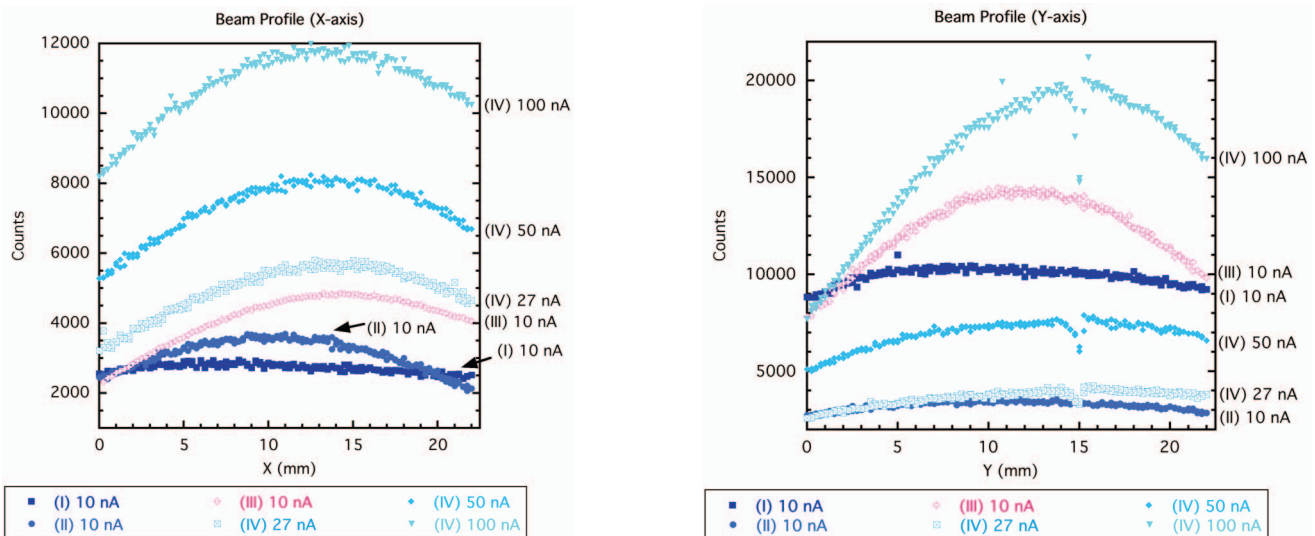


Fig. 6: Beam X (left) and Y (right) profiles measured on-line with the UniBeAM detector for different test sessions and beam currents.

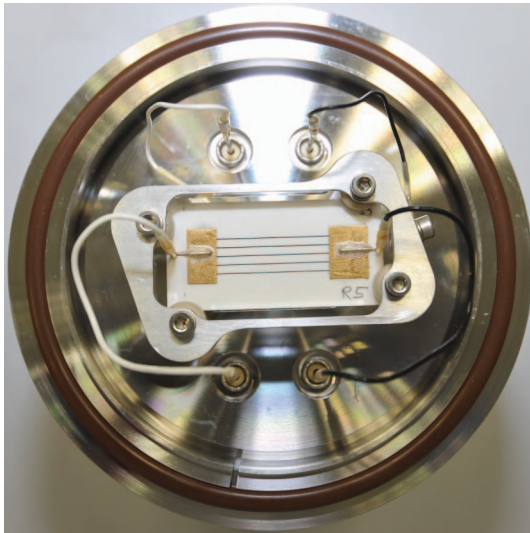


Fig. 7: Vacuum enclosure with one of the samples (#R-5) connected to the high-voltage power supply. Same configuration is used for #R-3.

observed. The irradiation is stopped immediately as the pressure rose to an unsafe value of $1.6 \cdot 10^{-5}$ mbar. The source of the outgassing is unknown, but to avoid vacuum problems the maximum current density for any subsequent irradiation is limited to $\sim 11 \text{ nA cm}^{-2}$ (second-last ramp in Fig. 10).

After the beam is stopped, the temperature profile during the sample's cooldown in vacuum is observed. Surprisingly, the sample temperature increases sharply from ~ 60 to $\sim 70 \text{ }^\circ\text{C}$ (Fig. 10) as soon as the beam line is vented with air at minute 40, before starting to decrease again. This behavior has been observed repeatedly also with other samples (Fig. 12 and 15) and is hypothesized to be due to transfer of heat from the beam dump, which is placed few mm behind the sample and most likely becomes hotter than the sample during the irradiation. When venting, this heat transfer by conduction in air is much more effective than by radiation in vacuum, hence the reason for the observed temperature increase.

Figure 8 shows #R-3 after irradiation. The ceramic substrate assumes a substantially brown color. Parts of the samples that are masked by thin PEEK rings (not thick enough to

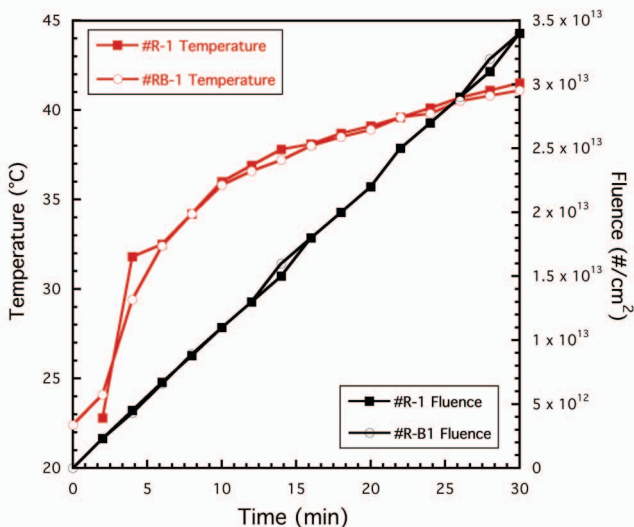


Fig. 9: Cumulative fluence and temperature measurement during constant beam current irradiation of #R-1 and #R-B1 samples.



Fig. 8: Front (left) and back (right) sides of #R-3 sample after irradiation.

completely stop the 18 MeV p^+) look substantially white. On the back side of the #R-1 samples, the lighter-brownish shadows of the connecting wires on the exposed side of the sample could be observed. Therefore, we conclude that the darkening of the ceramic substrate is due to radiation-induced modification of substances that accumulate during irradiation on sample's exposed surfaces.

The #R-3 samples shows a peculiar behavior after irradiation. When the resistance is measured by connecting the insulation tester at 50 V, then setting the instrument at 500 V, and again back at 50 V, the measurements (a, b, and c values in Table II) consistently show results of 16.1, 13.2, and 13.7 M Ω . If the insulation tester is disconnected and reconnected again after few minutes, the same pattern can be observed. This behavior is confirmed by repeating these measurement multiple times several days and weeks after irradiation. The sample seems to have undergone a permanent damage that seems to lead to sample charging that affects its resistance when repeatedly measured with the insulation tester.

#R-5 is the last irradiated sample, for a target fluence that is about double than #R-3's, with beam current density of $\sim 11 \text{ nA cm}^{-2}$ and +3.5 kV applied voltage. A failure of the electrometer monitoring the beam current after ~ 5 minutes, probably induced by a discharge forced us to continue the irradiation without a real-time measurement of the beam current, but only monitoring the beam line parameters. The current density can be assumed to have a larger variance, at about $11 \pm 2 \text{ nA cm}^{-2}$ for the duration of the irradiation. The resistance of the sample after irradiation is the same as before, even when repeated after 8 months. The peculiar behavior of #R-3 cannot be observed of this sample. Therefore, we conclude that the source of #R-3 behavior is not due to

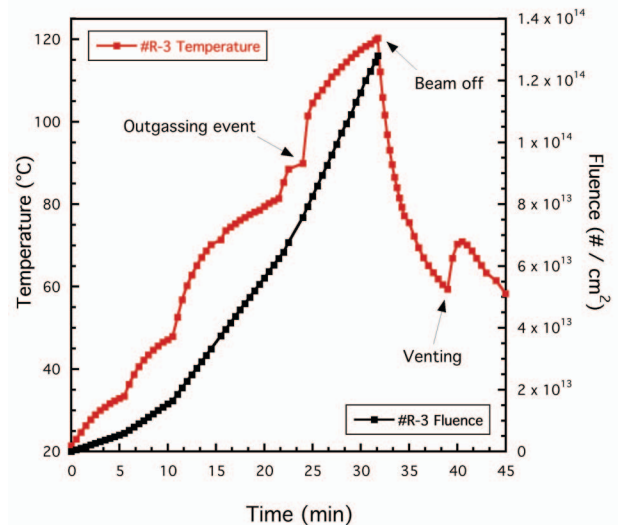


Fig. 10: Cumulative fluence and temperature measurement during variable beam current irradiation of #R-3 sample, including cooling curve.

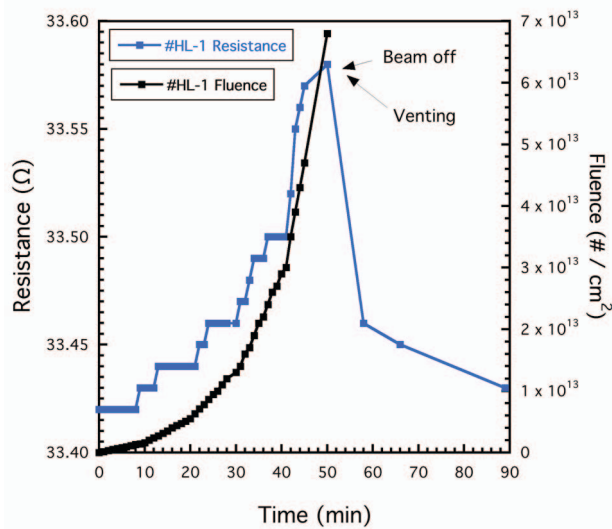


Fig. 11: Cumulative fluence and resistance measurement during variable beam current irradiation of #HL-1 sample.

damages to the resistor paste due to total dose, but rather by damages of the paste or its coating induced by the excessive flux that hit the sample during the last ramp of beam current, where both an anomalous temperature profile (Fig. 10) and an outgassing pressure spike was observed. Because the fluxes encountered in space are order of magnitudes lower than the one used for this accelerated experiment, we consider that the #R-3 damage is not a credible failure mode in space.

In summary, the DuPont 2051 paste is considered radiation hard up to a total dose of ~ 85 Mrad in space, which much higher than the target dose of ~ 15 Mrad Si (including margin of 4) expected for the JUICE mission at Jupiter.

C. Heater (#HL, DuPont 7410) Samples Irradiation

#HL-1 (32.1Ω) and #HL-B1 (1.6Ω) are irradiated with real-time monitoring of the sample resistance, to about the same total dose of #R-1 and #R-2.

The resistance of the #HL-1 sample increases during irradiation, for a maximum variation of $+0.15 \Omega$ (0.4%) just before switching off the beam (Fig. 11). 40 minutes after irradiation, the resistance returns to substantially the original value, and the observed profile of variation of the resistance can be ascribed to a positive temperature coefficient (α).

The resistance of #HL-B1, on the other side, decreases during irradiation, for a maximum variation of -0.0338Ω or 2% just before switching off the beam (Fig. 12). As soon as the beam is turned off, the resistance increases again stabilizing to a value that differs by less than 0.01% with respect to the value before irradiation. Therefore, we can consider both samples not permanently damaged by radiation.

The opposite temperature dependence of the two resistors during irradiation is worth commenting in more details. For #HL-B1, upon venting we observe a peak (Fig. 12) similarly as for #R-3 (Fig. 10), although this time the measured quantity is resistance and not temperature. This drop in the resistance of #HL-B1 as the sample is heated during venting demonstrates that for this sample $\alpha < 0$. It is interesting to note that the same resistor paste can lead to temperature

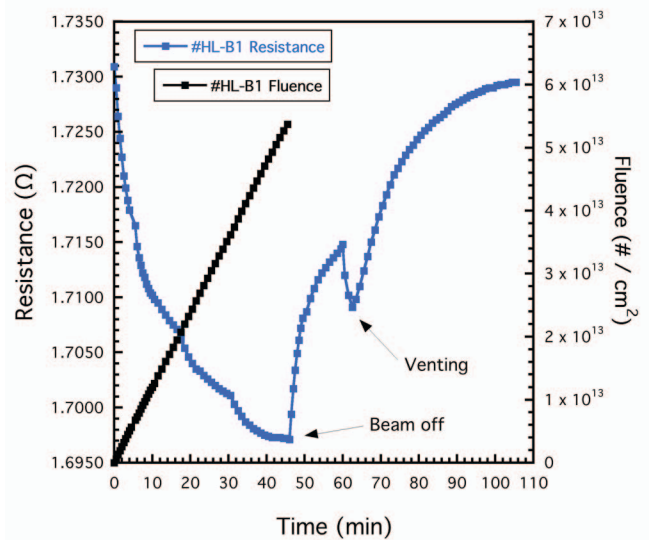


Fig. 12: Cumulative fluence and resistance measurement during constant beam current irradiation of #HL-B1 sample.

coefficients of different signs depending on the geometry of the printed resistors (in this case, multiple narrow versus one bold traces). This implies that it might be possible to print these resistors in geometries that allow achieving a temperature coefficient equal or close to zero, thus allow to print precision resistors for specific applications.

In summary, the DuPont 7410 paste is considered to be radiation hard up to a total dose of ~ 17 Mrad in space, which is more than double the target dose of ~ 8 Mrad Si (including margin of 4) expected for the JUICE mission at Jupiter.

D. Heater (#HH, DuPont 7499) Samples Irradiation

#HH-B2 (78.83Ω) and #HH-B3 (61.03Ω) are irradiated in the same conditions of #HL-1 and #HL-B1, respectively.

Both samples show a decrease in resistance during irradiation (Fig. 14 and 15), which can be ascribed to a negative temperature coefficient for the same reasons discussed earlier. Since both samples are of B-type, we cannot conclude whether narrow-traces samples would have a negative temperature coefficient, as it is the case for #HL samples.

The resistance of #HH-B2, increases after the beam is

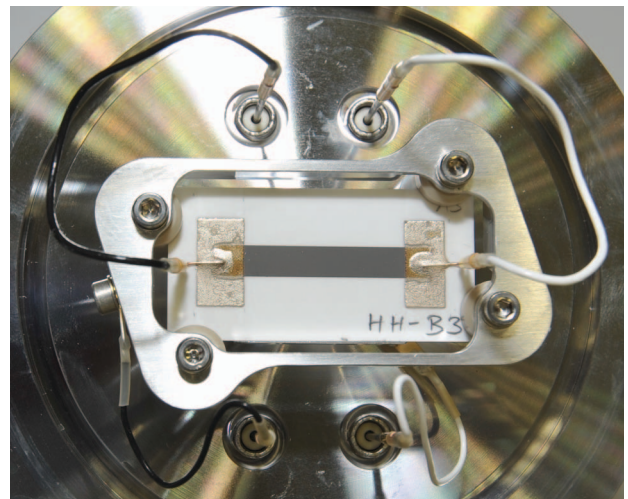


Fig. 13: #HH-B3 sample in the vacuum enclosure with real-time resistance measurement.

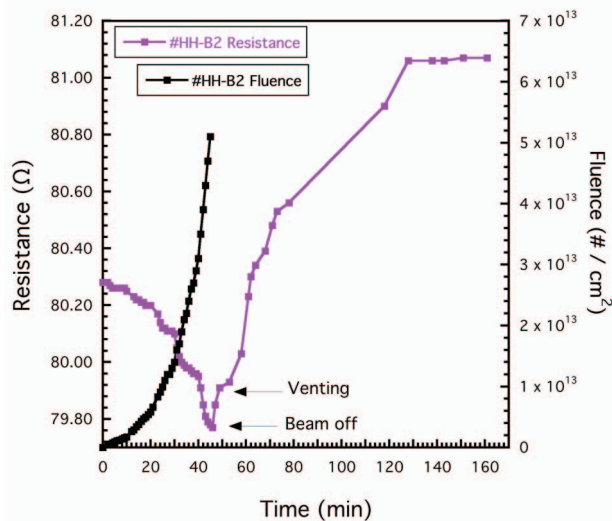


Fig. 14: Cumulative fluence and resistance measurement during variable beam current irradiation of #HH-B2 sample.

stopped and stabilizes to a value that is $\sim 1 \Omega$ higher (1% change) than the one before irradiation. The measurement performed at contact after irradiation (Table II) confirms the observation made with the long cables, thus pointing at a permanent damage of this samples due to the irradiation.

The resistance of #HH-B3, also increases after irradiation but seems to return to the pre-irradiation as it cools down. However, the sample shows a significant increase of the resistance to 65.56Ω (+4 Ω , +7% change) when re-measured at contact several months after irradiation.

Both these results show that both samples underwent permanent degradation of the resistance, up to plus several % of the original value, when irradiated to ~ 17 Mrad. It has to be noted that the lot of paste of DuPont 7499 employed for this test was significantly older (2008) than the lots used for 2051 and 7410 (2012), so we cannot exclude that the root cause of the radiation-induced degradation be shelf-life.

All in all, we still consider DuPont 7499 to be usable for the heater of the NIM instrument, as long as the heater power supply is designed to accounted for possible + $\sim 10\%$ variation of the resistance at mission end of life. Besides, as the resistance is increasing upon degradation by radiation, the risk of overcurrent on the heater is not increased even if the expected resistance variation exceeds the measured value.

IX. CONCLUSION

This study investigated with an 18 MeV proton beam the radiation hardness of three resistor pastes (DuPont 2051, 7410, and 7499) that are used to screen-print resistors employed in high-voltage ion optical elements and in decontamination heaters in the ion-optical system of the Neutral and Ion Mass spectrometer (NIM) of the Particle Environment Package (PEP) on the ESA JUICE mission.

This study demonstrates that DuPont 2051 and 7410 are radiation hard up to ~ 85 and 17 Mrad, respectively, thus complying with the expected Total Ionizing Dose (TID) of the JUICE mission with a radiation margin of $\sim 22x$ and $\sim 9x$, respectively. DuPont 7499 shows a permanent increase of the

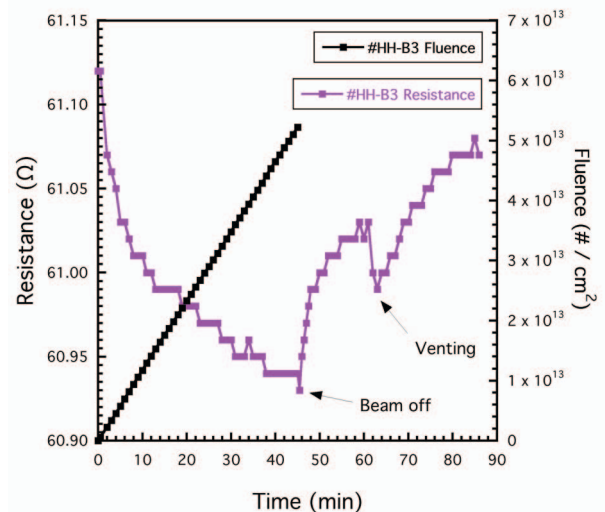


Fig. 15: Cumulative fluence and resistance measurement during constant beam current irradiation of #HH-B3 sample.

resistance of ~ 1 – 7% after irradiation to ~ 17 Mrad, although the fact that the lot employed was very old does not allow to draw a conclusive statement on the radiation hardness of this material.

This study also shows that permanent damages to the samples, with associated outgassing, can be incurred for beam current densities exceeding $\sim 10 \text{ nA cm}^{-2}$ and temperature beyond $\sim 100 \text{ }^\circ\text{C}$, thus showing the importance of monitoring the sample temperature and the beamline pressure during irradiation.

In summary, this study demonstrates that all investigated materials underwent no or acceptable degradation after irradiation with 18 MeV protons up to target doses that largely exceed those expected for these material space, and it is of utmost importance to confirm that the selected technological baseline of NIM is compatible with Jupiter environment. Besides, it provides the grounds for the potential implementation of these materials for high-voltage ion-optical elements and heaters on space and ground instrumentation bound to work in a harsh radiation environment. Finally, this study proves that the employed cyclotron facility – conceived for the synergic execution of both medical radioisotope production and applied research on materials, detectors, and devices – can be effectively used also for assessing the radiation hardness or materials for space applications.

X. ACKNOWLEDGMENT

The authors thank Daniele Piazza, Matthias Lüthi, Jürg Jost, Christoph Josi, and Michael Gerber for their support in engineering the irradiation station and during measurements.

XI. REFERENCES

- [1] "JUICE environment specification", ESA, Noordwijk, The Netherlands, Rep. JS-14-09 v5.4, Jun. 20, 2015.
- [2] S. Meyer, M. Tulej, and P. Wurz, "Mass spectrometry of planetary exospheres at high relative velocity: direct comparison of open- and closed source measurements," *Geosci. Instr. Method. Data Syst.* 6(1), (2017) 1-8, doi:10.5194/gi-2016-28.

- [3] Barabash, S. et al., 2013. Particle Environment Package (PEP). European Planetary Science Congress 2013, held 8–13 September in London, UK, vol. 8. EPSC2013.
- [4] M. Tulej, S. Meyer, M. Lüthi, D. Lasi, A. Galli, L. Desorgher, W. Hajdas, S. Karlsson, L. Kalla, and P. Wurz, "Detection efficiency of microchannel plates for e^- and π^- in the momentum range from 17.5 to 345 MeV/c," *Rev. Sci. Instrum.*, vol. 86, pp. 083310-1–083310-12, Aug. 2015.
- [5] M. Tulej, S. Meyer, M. Lüthi, D. Lasi, A. Galli, D. Piazza, L. Desorgher, D. Reggiani, W. Hajdas, S. Karlsson, L. Kalla and P. Wurz, "Experimental investigation of the radiation shielding efficiency of a MCP detector in the radiation environment near Jupiter's moon Europa," *Nucl. Instr. Meth. B*, vol. 383, pp. 21–37, Sep. 2016.
- [6] D. Lasi, M. Tulej, S. Meyer, M. Lüthi, A. Galli, D. Piazza, P. Wurz, D. Reggiani, H. Xiao, R. Marcinkowski, W. Hajdas, A. Cervelli, S. Karlsson, T. Knight, M. Grande, and S. Barabash, "Shielding an MCP detector for a space-borne mass spectrometer against the harsh radiation environment in Jupiter's Magnetosphere," *IEEE Trans. Nucl. Sci.* 64(1), (2017), 605-613, DOI: 10.1109/TNS.2016.2614040.
- [7] H. Balsiger, K. Altwegg, P. Bochsler, P. Eberhardt, J. Fischer, S. Graf, A. Jäckel, E. Kopp, U. Langer, M. Mildner, J. Müller, T. Riesen, M. Rubin, S. Scherer, P. Wurz, S. Wüthrich, E. Arijis, S. Delanoye, J. De Keyser, E. Neefs, D. Nevejans, H. Rème, C. Aoustin, C. Mazelle, J.-L. Médale, J.A. Sauvaud, J.-J. Berthelier, J.-L. Bertaux, L. Duvet, J.-M. Illiano, S.A. Fuselier, A.G. Ghielmetti, T. Magoncelli, E.G. Shelley, A. Korth, K. Heerlein, H. Lauche, S. Livi, A. Loose, U. Mall, B. Wilken, F. Gliem, B. Fiethe, T.I. Gombosi, B. Block, G.R. Carignan, L.A. Fisk, J.H. Waite, D.T. Young, and H. Wollnik, "ROSINA - Rosetta Orbiter Spectrometer for Ion and Neutral Analysis," *Space Sci. Rev.* 128 (2007), 745-801.
- [8] L. Hofer, P. Wurz, A. Buch, M. Cabane, P. Coll, D. Coscia, M. Gerasimov, D. Lasi, A. Saggir, C. Szopa, and M. Tulej, "Prototype of the gas chromatograph - mass spectrometer to investigate volatile species in the lunar soil for the Luna-Resurs mission," *Planet. Space Sci.*, 111 (2015) 126-133.
- [9] <http://www.dupont.com/products-and-services/electronic-electrical-materials/hybrid-circuit-materials/products/thick-film-resistor-materials.html>
- [10] S. Scherer, K. Altwegg, H. Balsiger, J. Fischer, A. Jäckel, A. Korth, M. Mildner, D. Piazza, H. Rème, and P. Wurz, "A novel principle for an ion mirror design in time-of-flight mass spectrometry," *Int. J. Mass Spectrom.* 251 (2006) 73-81.
- [11] C. Leinenbach, N. Weyrich, H.R. Elsener, G. Gamez, *Int. J. Appl. Ceram. Tec.*, 9 [4] 751–763 (2012)
- [12] S. Braccini, The new Bern PET cyclotron, its research beam line, and the development of an innovative beam monitor detector, *AIP Conf. Proc.* 1525 (2013) 144-150.
- [13] M. Auger, S. Braccini, A. Ereditato, K.P. Nesteruk and P. Scampoli, Low current performance of the Bern medical cyclotron down to the pA range, *Meas. Sci. Technol.* 26 (2015) 094006.
- [14] S. Braccini and P. Scampoli, Science with a medical PET cyclotron, *CERN Courier* 56 (2016) 21.
- [15] Riedo, A., Neuland, M., Meyer, S., Tulej, M., Wurz, P., "Coupling of LMS with a fs-laser ablation ion source: elemental and isotope composition measurements", *J. Anal. At. Spectrom.*, 28 (2013), 1256-1269.
- [16] M. J. Berger, J. S. Coursey, M. A. Zucker, and J. Chang, "ESTAR, PSTAR, and ASTAR: Computer Programs for Calculating Stopping-Power and Range Tables for Electrons, Protons, and Helium Ions," version 1.2.3, National Institute of Standards and Technology, Gaithersburg, MD, 2005. [Online] Available: <http://physics.nist.gov/PhysRefData/Star/Text/ESTAR.html>. Accessed on: Aug. 20, 2016.
- [17] Ziegler, J.F., Ziegler, M.D., Biersack, J.P., 2010. SRIM - The stopping and range of ions in matter, *Nucl. Instr. Meth. Phys. Res. B*, Volume 268, Issue 11-12, p. 1818-1823